Paleoceanography and Paleoclimatology

RESEARCH ARTICLE
10.1029/2017PA003312

Key Points:
- North Atlantic deep ocean calcite saturation is reconstructed using B/Ca ratios in benthic foraminifera across the mid-to-late Pleistocene
- Deep ocean ΔCO_3^{2-} levels declined across the mid-Pleistocene, and G/IG ΔCO_3^{2} amplitude increased as ΔCO_3^{2} became persistently undersaturated 400 kyr ago
- Shifts in the locus of $CaCO_3$ burial maintain the global $CaCO_3$ balance on G/IG timescales

Supporting Information:
- Supporting Information S1
- Table S1

Correspondence to:
S. M. Sosdian,
sosdians@cardiff.ac.uk

Citation:
Sosdian, S. M., Rosenthal, Y., & Toggweiler, J. R. (2018). Deep Atlantic carbonate ion and $CaCO_3$ compensation during the ice ages. *Paleoceanography and Paleoclimatology*, *33*, 546–562. https://doi.org/10.1029/2017PA003312

Received 20 DEC 2017
Accepted 7 APR 2018
Accepted article online 16 APR 2018
Published online 4 JUN 2018

Deep Atlantic Carbonate Ion and $CaCO_3$ Compensation During the Ice Ages

S. M. Sosdian[1], Y. Rosenthal[2,3], and J. R. Toggweiler[4]

[1]School of Earth and Ocean Sciences, Cardiff University, Cardiff, UK, [2]Department of Marine and Coastal Sciences, Rutgers University, New Brunswick, NJ, USA, [3]Department of Earth and Planetary Sciences, Rutgers University, New Brunswick, NJ, USA, [4]Geophysical Fluid Dynamics Laboratory, NOAA, Princeton, NJ, USA

Abstract Higher alkalinity compensates for reduced $CaCO_3$ burial in the deep ocean in response to increased carbon sequestration. This process could account for about half of the reduction in glacial atmospheric CO_2. To date, our understanding of this process comes from benthic carbon isotope and $CaCO_3$ burial records. Here we present a 1.5 Myr orbitally resolved deep ocean calcite saturation record (ΔCO_3^{2-}) derived from benthic foraminiferal B/Ca ratios in the North Atlantic. Glacial ΔCO_3^{2-} declines across the mid-Pleistocene transition suggesting increased sequestration of carbon in the deep Atlantic. The magnitude, timing, and structure of deep Atlantic Ocean ΔCO_3^{2-} parallel changes in $\%CaCO_3$ and contrasts with the small amplitude, anti phased swings in Indo-Pacific ΔCO_3^{2-} and $\%CaCO_3$ during the mid-to-late Pleistocene questioning the classic view of $CaCO_3$ compensatory mechanism. We propose that the increasing corrosivity of the deep Atlantic causes the locus of $CaCO_3$ burial to shift into the equatorial Pacific where the flux of $CaCO_3$ to the seafloor was sufficiently high to overcome low saturation and establish a new burial "hot spot." Based on this mechanism, we propose that the persistently lowΔCO_3^{2-} levels at marine isotope stage 12 set the stage for the high pCO_2 levels at marine isotope stage 11 and subsequent interglacials via large swings in ocean alkalinity caused by shifts in $CaCO_3$ burial. Similarly, the development of classic ("anticorrelated") $CaCO_3$ patterns was driven by enhanced ocean stratification and an increase in deep ocean corrosivity in response to mid-Pleistocene transition cooling.

1. Introduction

Mechanisms proposed to explain Pleistocene changes in atmospheric carbon dioxide (pCO_2) call for a transfer of carbon dioxide from the atmosphere to the glacial deep ocean by way of increased efficiency of the biological pump (Boyle, 1988; Broecker & Peng, 1982, 1987). In contrast, upwelling of respired CO_2 and its transfer back to the atmosphere would explain the pCO_2 increase during the interglacials. However, as previously pointed out biological mechanisms cannot account for the full glacial/interglacial (G/IG) amplitude and duration of atmospheric pCO_2 during the late Pleistocene (Archer & Maierreimer, 1994; Boyle, 1988; Broecker & Peng, 1982, 1989; Sigman & Boyle, 2000; Toggweiler, 1999). This raises the likelihood that calcium carbonate ($CaCO_3$) compensation in response to changes in the amount of carbon sequestered in the deep ocean might have had a substantial contribution to the G/IG changes in pCO_2 (Boyle, 1988; Broecker & Peng, 1982; Broecker & Peng, 1987; Toggweiler, 1999).

In this scenario, the sequestration of excess glacial metabolic CO_2 reduces carbonate ions (CO_3^{2-}) in the deep ocean. As the deep ocean CO_3^{2-} is controlled by the balance between the supply of ingredients for $CaCO_3$ (calcium [Ca^{2+}] and bicarbonate [HCO_3^{-}]) into the ocean and removal via burial of $CaCO_3$ in the sediments, this imbalance promotes $CaCO_3$ dissolution until a new steady state is reached via adjustments in the lysocline, the depth in the ocean where $CaCO_3$ preservation (above) gives way to dissolution (below). The shoaling of the lysocline raises ocean alkalinity and acts to further lower atmospheric pCO_2. Current $CaCO_3$ compensation theory predicts that the ocean CO_3^{2-} response should be fairly fast, within the range of 5–10 kyr and atmospheric pCO_2 would change on the timescale set by the CO_3^{2-} response time (Archer et al., 1997; Broecker & Peng, 1987; Keir, 1988; Köhler & Fischer, 2006). If this mechanism did operate on G/IG timescales across the Pleistocene, we would expect to find evidence for relevant oscillations in deep ocean carbon storage, CO_3^{2-} content, and lysocline in tandem with $CaCO_3$ preservation, and dissolution patterns.

A second mechanism proposed to explain G/IG changes in deep ocean CO_3^{2-} and $CaCO_3$ burial patterns invokes sea level-driven shifts in carbonate deposition a.k.a. coral reef hypothesis (Berger, 1982; Berger &

Keir, 1984; Opdyke & Walker, 1992). In this scenario, during glaciation, sea level drop reduces the shelf area and $CaCO_3$ deposition on continental shelves. This would act to increase whole ocean alkalinity and deep ocean CO_3^{2-} and plays a critical role in reducing atmospheric pCO_2. This idea implies that on G/IG timescales whole ocean alkalinity and pCO_2 are dictated by sea level-driven shifts in the partitioning of $CaCO_3$ deposition between the continental shelf and deep ocean, or more specifically enhanced glacial preservation is tied to alkalinity supplied from the shelf areas during this period of sea level fall. If this hypothesis did operate on G/IG timescales, then there should be a correlation between the timing and amplitude of long-term changes in deep ocean CO_3^{2-} and sea level in the past.

Most of our knowledge for changes in Pleistocene deep ocean G/IG carbon inventory and sedimentary carbonate processes derives from benthic carbon isotope records ($\delta^{13}C_b$) and $CaCO_3$ burial and preservation fluxes. $\delta^{13}C_b$ records have been used to track the transfer of carbon between the organic and inorganic pools in the ocean, and records spanning the Pleistocene have also been interpreted to reflect large G/IG shifts in water mass distributions with implications for carbon storage in the deep ocean (Clark et al., 2006; Raymo et al., 1997; Skinner, 2009). However, interpretations of $\delta^{13}C_b$ records in terms of carbon storage and circulation are confounded as these proxies are impacted by a range of biogeochemical and physical processes, such as changes in preformed $\delta^{13}C_b$ signals of the source water (Lynch-Stieglitz et al., 1995; Raymo et al., 1997; Yu et al., 2008, and references herein). Pleistocene $\%CaCO_3$ records from the deep Atlantic show enhanced dissolution during glacial periods relative to interglacials, whereas Pacific $\%CaCO_3$ records indicate enhanced preservation during glacials relative to interglacials (Arhenius, 1952; deMenocal et al., 1997; Farrell & Prell, 1989; Howard & Prell, 1994; Hodell, Charles, & Sierro, 2001; Sexton & Barker, 2012, and references here in). This classic "seesaw" $CaCO_3$ preservation pattern has persisted across the last 800 kyr and has been suggested to vary in response to the vertical repositioning of the Atlantic lysocline (Berger & Winterer, 1974; Boyle, 1983; deMenocal et al., 1997; Farrell & Prell, 1989; Howard & Prell, 1994). However, interpretations of $\%CaCO_3$ records in terms of variations of deep ocean CO_3^{2-} are confounded by the fact that in addition to dissolution, they also reflect carbonate production and dilution by terrigenous material and thus cannot directly be related to changes in atmospheric pCO_2.

A robust assessment of deep ocean CO_3^{2-} across Pleistocene G/IG cycles awaits the development of basin-wide records of ocean carbonate chemistry to fully resolve the nature of the ocean buffering capacity and its role in driving G/IG pCO_2 cycles. As the CO_3^{2-} of the deep ocean is regulated by changes in mean ocean alkalinity, records of deep ocean CO_3^{2-} and $\%CaCO_3$ provide insights into the compensation mechanism, coral reef hypothesis, and the ability of the ocean to buffer changes in atmospheric CO_2. Also, the CO_3^{2-} of the deep ocean's respired carbon pool should track atmospheric pCO_2, which makes it a good proxy to investigate mechanisms affecting the carbon cycle and atmospheric pCO_2 (Broecker & Peng, 1987; Yu et al., 2010). Here we use boron to calcium ratios in the benthic foraminifer *Cibicidoides wuellerstorfi* as a means to investigate Pleistocene G/IG changes in deep North Atlantic Ocean CO_3^{2-}.

Boron to calcium (B/Ca) ratios in epifaunal benthic foraminifera have been used to reconstruct seawater calcite saturation state ($\Delta[CO_3^{2-}] = [CO_3^{2-}{}_{in\ situ}] - [CO_3^{2-}{}_{sat}]$) based on available empirical calibrations (Brown et al., 2011; Rae et al., 2011; Raitzsch et al., 2011; Yu et al., 2013; Yu & Elderfield, 2007). Overall, the available evidence from B/Ca-based ΔCO_3^{2-} records show a divergent response related to depth and ocean basin across the last glacial cycle (Allen et al., 2015; Doss & Marchitto, 2013; Yu et al., 2010, 2013, 2014, 2016). Currently available, long Pleistocene records are mostly of low resolution documenting long-term trends in ΔCO_3^{2-} but not resolving the G/IG cyclicity (Elmore et al., 2015; Kender et al., 2016; Rickaby et al., 2010) except for two recent studies. In the North Atlantic, Lear et al. (2016) put forth a suite ($n = 80$) of trace metal records (Cd/Ca, B/Ca, and U/Ca) across the mid-Pleistocene (0.4 to 1.1 Ma) from Deep Sea Drilling Program (DSDP) Site 607 and show a decrease in glacial B/Ca values across the mid-Pleistocene transition (MPT). As G/IG changes in $\delta^{13}C_b$ occur alongside shifts in nutrient content and deep ocean CO_3^{2-}, the authors attributed the cause to a change from dominantly northern water mass to dominantly southern source waters across the MPT and an increase in respired carbon pool of the glacial Atlantic. Beyond this they suggest that the increased corrosivity of bottom waters during glacials might have increased mean ocean alkalinity and lowered atmospheric pCO_2 (Lear et al., 2016). Additionally, a study by Kerr et al. (2017), using orbitally resolved Indo-Pacific B/Ca records show that deep Pacific CO_3^{2-} concentration slightly increased during the glacial intervals while falling during the interglacials across the last 500 kyr with similar patterns to the

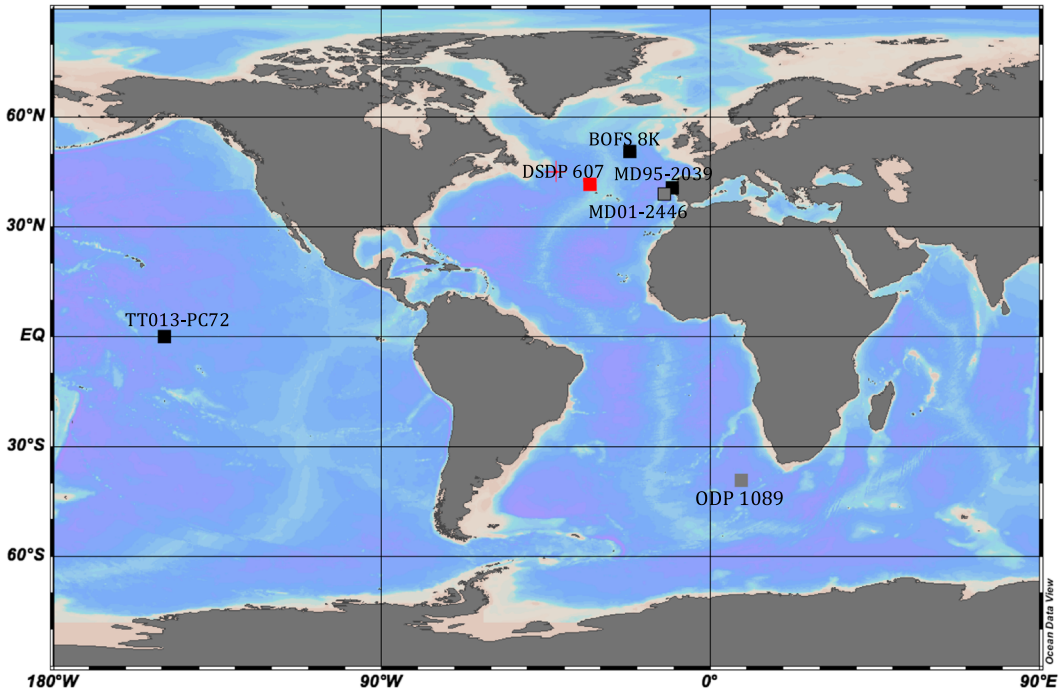

Figure 1. Ocean data viewer bathymetric map showing modern locations of Deep Sea Drilling Program (DSDP) Site 607 (depth = 3.4 km; red symbol) used in this study and from previously published data (grey/black symbols; BOFS8K depth = 4.0 km; MD95-2039 depth = 3.4 km; MD01-2446 depth = 3.6 km; ODP 1089 depth = 4.6 km; TT013-PC72 depth = 4.3 km) (Schlitzer, 2012).

sediment $CaCO_3$ content. They argue that a global increase in CO_3^{2-} during glacial intervals is caused by the reduction of carbonate deposition on the shelves during low sea level stands (a.k.a. "coral reef hypothesis") across the last 450 kyr (Berger, 1982; Opdyke & Walker, 1992). Here we explore alternative mechanism, whereby the post-MPT Pacific and Atlantic CO_3^{2-} records are driven by shifts in the locus of $CaCO_3$ burial.

In this paper we extend the DSDP Site 607 North Atlantic record of Lear et al. (2016; n = 80) and increase the number of samples by 275 analyses, alongside including a nearby piston core record (Chain 84-24-23 PC) to provide a complete orbitally resolved benthic foraminifera B/Ca reconstruction for the last 1.5 Myr through the mid-to-late Pleistocene. Combined with existing Indo-Pacific B/Ca records (Kerr et al., 2017), carbon isotope, and %$CaCO_3$ records (Raymo et al., 1997; Ruddiman et al., 1989), we investigate mechanisms controlling the deep ocean carbon budget of the North Atlantic and examine the physical and biogeochemical processes that can explain the observed G/IG changes in ΔCO_3^{2-}. The focus on the deep Atlantic stems from geochemical and modeling evidence suggesting the deep North Atlantic has played a significant role in carbon sequestration on G/IG timescales during the late Pleistocene (Hain et al., 2010; Howe et al., 2016; Toggweiler, 1999; Yu et al., 2016). We discuss the importance of the $CaCO_3$ cycle for the G/IG pCO_2 change in light of this 1.5 Myr Atlantic ΔCO_3^{2-} stack and propose that the enhancement of atmospheric pCO_2 by $CaCO_3$ compensation is due to a change in the locus of $CaCO_3$ burial between the Atlantic and Indo-Pacific in response to the transfer of alkalinity between these ocean basins. Our new record also provides new insights into the mechanisms associated with the MPT and mid-Brunhes event.

2. Core Material and Methods

2.1. Hydrographic Conditions and Age Model

We present benthic foraminiferal B/Ca records for DSDP Site 607 (41°00′N, 32°57′W, 3,427 m) on the western flank of the Mid-Atlantic Ridge supplemented with measurements from a nearby piston core (Chain 82-24-23 Piston Core (referred to hereafter as CHN82-24-23PC; 43°N, 31°W; water depth 3,406 m; Figure 1). Both sites are situated within the path of North Atlantic Deep Water (NADW; T = 2.6 °C, S = 34.1) close to its northern

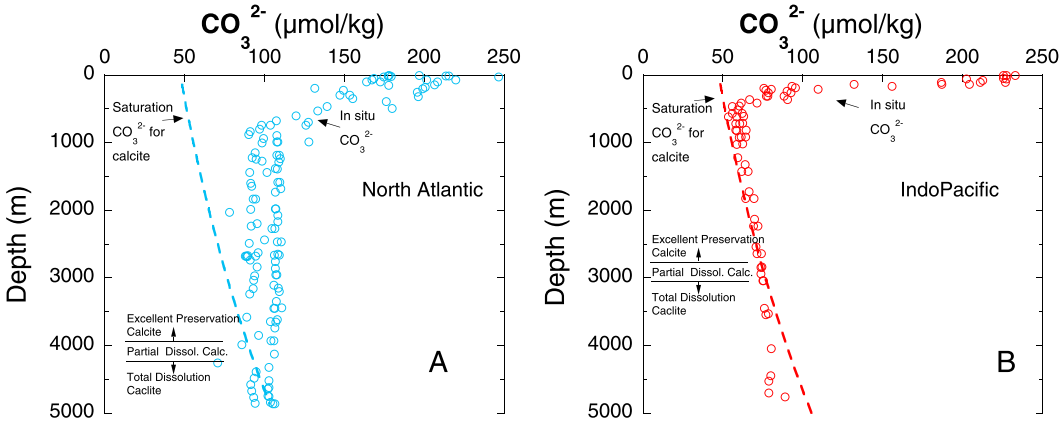

Figure 2. Deep CO_3^{2-} profiles from (a) the North Atlantic near Deep Sea Drilling Program Site 607 and (b) equatorial Indo-Pacific, nearby Site TT013-PC72, used in Kerr et al. (2017) B/Ca record. In the modern ocean, basin-specific differences in deep ocean CO_3^{2-} occur as a result of the formation of North Atlantic Deep Water, which fills the deep Atlantic today with preservation-friendly, high-CO_3^{2-} water whereas the deep Pacific is filled with corrosive low-CO_3^{2-} water in response. The saturation state ($\Delta[CO_3^{2-}]$) of the deep ocean modulates the depth in the ocean where $CaCO_3$ preservation (above) gives way to dissolution (below) termed the lysocline whereby its position is deeper in the Atlantic with more $CaCO_3$ burial per unit area relative to the Pacific (Dunne et al., 2012). Carbonate system data are from nearby GLODAP Sites (Key et al., 2004).

sources. In the modern ocean, bottom water at these sites reflects the influence of mostly of NADW (low nutrient, high $\delta^{13}C_b$, and ΔCO_3^{2-}) and to a lesser extent Antarctic Bottom Water (AABW; enriched nutrient, low $\delta^{13}C_b$, and ΔCO_3^{2}; Yu et al., 2008; Figure 2). Modern ΔCO_3^{2} (33.2 µmol/kg) are estimated from nearby GLODAP data (Key et al., 2004). The age model for both sites are based on LRO4 stack Lisiecki and Raymo (2005) and previously used in Sosdian and Rosenthal (2009).

2.2. Analytical Method

Well-preserved benthic foraminifera of the species *Cibicidoides wuellerstorfi* were picked from the >150 µm fraction at sampling intervals of 15 cm providing an average temporal resolution of ~3 kyr. Picked samples restricted to the morphology of *C. wuellerstorfi* sensu stricto for B/Ca analyses throughout the core (Rae et al., 2011). Pleistocene records of B/Ca should mainly reflect deep ocean ΔCO_3^{2-} variability due to the relatively long oceanic residence time of B (~10 Myr) and Ca (~1 Myr) and their conservative nature (Lemarchand et al., 2002). *Cibicidoides wuellerstorfi* B/Ca were converted to deep sea ΔCO_3^{2-} using a sensitivity of 1.14 µmol/mol per µmol/kg specific to this species obtained from the global core-top calibration from Yu and Elderfield (2007) where B/Ca (µmol/mol) = 1.14(±0.04) × ΔCO_3^{2-} (µmol/kg) +177(±1.0).

Samples were gently crushed between two glass plates, and metal oxides visible within chambers were removed from the sample to minimize contamination. The fragments were transferred into acid-cleaned, dry 0.5 ml microcentrifuge tubes. Crushed foraminiferal samples contained 3–15 individuals and ideally weighed from 0.200 to 0.400 mg, but due to low species abundance in certain intervals samples occasionally weighed <0.200 mg. Samples were cleaned using the reductive or "long" cleaning protocol (Boyle and Keigwin, 1985; Rosenthal et al., 1997). The effect of different cleaning methods on B/Ca ratios is minimal (Yu & Elderfield, 2007). Samples were cleaned and dissolved using reagents prepared with boron-free water as prepared by passing double distilled water over an anion exchange resin (Aldrich, amberlite IRA-743) to remove boron. Following cleaning, samples were dissolved in trace metal clean 0.065 N nitric acid (SEASTAR) and 100 µl of this solution was diluted with 300 µl of trace metal clean 0.5 N nitric acid to obtain a Ca concentration of about 3 ± 1 mmol/mol. Diluted samples were analyzed for a suite of trace metal ratios using the Rutgers sector field inductively coupled plasma-mass spectrometer , on a Finnigan MAT Element-1 and Element-2 XR located at the Department of Marine and Coastal Sciences using methods adapted from Rosenthal et al. (1999). The method was slightly modified to accommodate for measurement of B/Ca ratios; specifically, ammonia gas was introduced in the Teflon-spray chamber during sample analysis to remove the memory effect associated with analysis of boron (Babila et al., 2014). Long-term precision, based on analysis of consistency

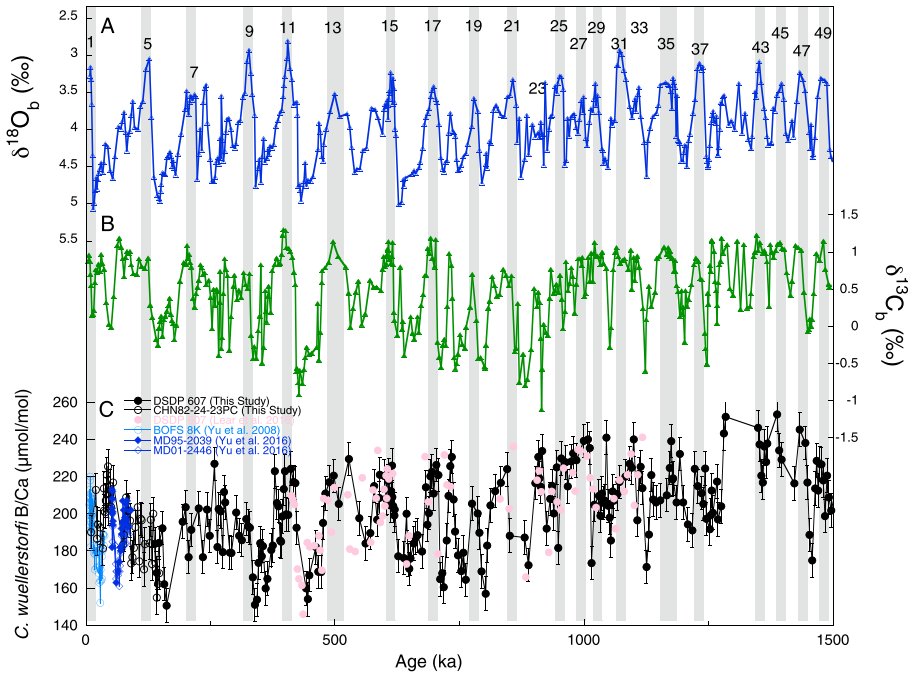

Figure 3. Deep Sea Drilling Program (DSDP) Site 607 records of benthic foraminiferal (a) $\delta^{18}O$ and (b) $\delta^{13}C$ (Ruddiman et al., 1989) and (c) B/Ca ratios from this study (DSDP 607 and CHN82-24-23PC) and previously published deep North Atlantic records from BOFS 8K (Yu et al., 2008), MD95-2039 (Yu et al., 2016), MD01-2446 (Yu et al., 2016), and DSDP Site 607 (Lear et al., 2016). All records are on the LRO4 age model, and MIS are highlighted based on LRO4 stack alignment (Lisiecki & Raymo, 2005). The error bars show analytical precision for B/Ca (r.s.d. = 4.0%).

standards across a range of B/Ca ratios is ±4%. Analysis runs including CHN82-24-23PC B/Ca records were offset from the long-term mean B/Ca, as determined by the long-term average of the consistency standards, and to account for this, we applied an analytical offset to CHN82-24-23PC B/Ca values of 5% prior to including them in Figure 3. Al and Ti were used as contaminant indicators, and no long-term correspondence in trend exists between B/Ca and each elemental ratio. However, across marine isotope stage (MIS) 25, high B/Ca values correspond with elevated Al and Ti and were removed from the final record.

2.3. Cross-Spectral Analysis and Trends in Glacial and Interglacial Maxima

Here we use the ARAND package (Howell et al., 2006) to evaluate the phase and coherency between elemental and isotopic records from DSDP 607 and compare variables relative to benthic $\delta^{18}O$ in 100-kyr world (i.e., from 140 to 750 ka, 100 kyr periodicity). We interpolated all records to even intervals of 3-kyr resolution prior to cross-spectral analysis and used the inverse of benthic $\delta^{18}O$ in the analysis. Proxy phase relationships are compared and presented in the representative time window during the "100-kyr world" of the late Pleistocene.

To explore the trends in glacial and interglacial extremes in B/Ca ratios, we define glacial and interglacial maxima across the last 1.5 Myr from the benthic oxygen isotope record. B/Ca maxima and minima were picked within a 10 ka window around the interglacial or glacial peak. This allows for uncertainty associated with identifying the interglacial or glacial maxima for each site and to account for changes in the nature of interglacial periods (Tzedakis et al., 2009). G-I amplitude is taken as the absolute value of the difference between successive average glacial/interglacial values (e.g., G1-IG1, G2-IG1, and G2-IG2).

3. Results

3.1. Down Core B/Ca Record

During the last 1.5 Myr, *C. wuellerstorfi* B/Ca at Site 607 exhibits G/IG variability with a decrease in average B/Ca of 21 μmol/mol across the Pleistocene. This is mostly driven by changes in the glacial values primarily decreasing at MIS 23 from 180 μmol/mol to an average 161 across MIS 20–18. Glacial B/Ca then increase

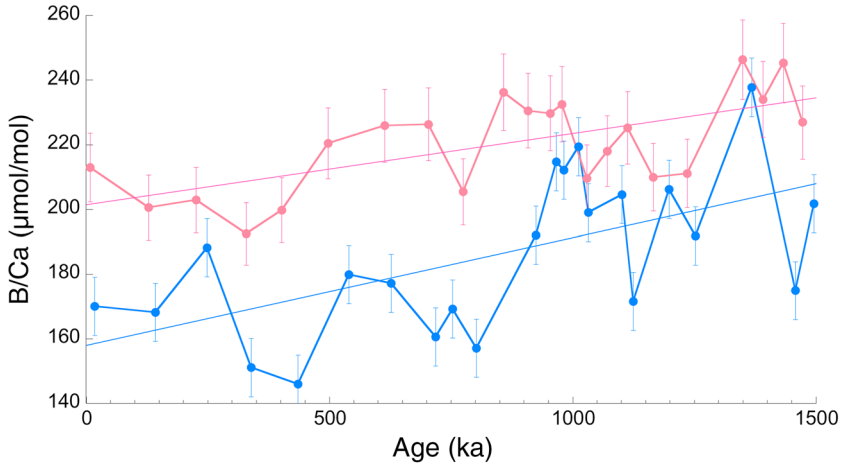

Figure 4. Interglacial and glacial B/Ca trends across the mid-to-late Pleistocene determined from the composite Deep Sea Drilling Program 607 and CHN82-24-23PC records. Data from BOFS 8K are used to estimate G/IG change across the H-LGM. The linear trends showcase the overall long-term decrease in interglacial and glacial B/Ca values. Note the steeper decrease in glacial relative to interglacial B/Ca values.

to 179 μmol/mol at MIS 14. At MIS 12, glacial B/Ca values decrease by 25 μmol/mol and persists at this level also during MIS 10 and 6 (Figures 3c and 4). In contrast, interglacial B/Ca ratios show a small long-term decline throughout the record. This results in G/IG amplitude that varies across the Pleistocene; during the pre-MPT interval (MIS 49 to 25, 1,500 to 950 ka), the average G/IG amplitude in B/Ca is ~24 μmol/mol (IG: 227 ± 4; G: 203 ± 5; ±1 standard errors of the mean, SEE). The G/IG amplitude increases to 48 (IG: 224 ± 3; G: 170 ± 1; ±1 SEE) μmol/mol across MIS 23 to 13 and throughout the late Pleistocene interval. Interglacial B/Ca values decrease at MIS 23 from average steady values of 227 to 206 μmol/mol at MIS 19 and increase at MIS 17 to average IG value of 227 μmol/mol. At MIS 11 it declines to an average IG value of 200 μmol/mol where it remains steady for the rest of the Pleistocene (Figure 4). Notably, the B/Ca record shows a remarkable correlation with the benthic foraminiferal $\delta^{13}C$ record on both G/IG and longer timescales (Ruddiman et al., 1989; Figures 3b and 3c).

Our piston core record encompasses the 165 to 75 ka and 55 to 10 ka interval. The CHN82-24-23PC B/Ca variability generally agrees with available records across these overlapping time intervals. For comparison, we look toward the published *C. wuellerstorfi* B/Ca records from Yu et al. (2008, 2016) from the deep North Atlantic across the Last Glacial Maximum (LGM) to Holocene (BOFS 8K; water depth 4,045 m) and from 60 to 90 ka (MD95-2039 and MD01-2446; Figure 3c). CHN82-24-23PC B/Ca tracks the rise to MIS 5 and decline into MIS 4 as shown in records from MD01-2446 and MD95-2039. The BOFS 8K record shows a similar amplitude change in B/Ca (ΔG/IG = 43, IG: 213, and G:170) μmol/mol to the G/IG change exhibited across the last 400 kyr from Site 607 (Figure S3). LGM CHN82-24-23PC B/Ca values do not reach the low values of BOFS 8K as the record is of lower resolution and likely not capturing the minimum in B/Ca.

The record of deep Atlantic B/Ca at Site 607 from this study agrees well with the lower resolution MPT record presented by Lear et al. (2016; Figure 3c). Therefore, we compile their data alongside our record and use this to examine the spectral properties of the record alongside examining deep ocean ΔCO_3^{2-} changes. The B/Ca record exhibits orbital frequencies similar to the $\delta^{18}O$ record with a strong 100 kyr peak present in the 140 to 700 ka time interval, following the MPT (Figure S2). Prior to the MPT, from 1,000 to 1,500 ka, the record shows precession-like periodicities (18, 21 kyr) but does not resolve a 41 kyr cyclicity, possibly due to small gaps in the record. Also, B/Ca changes lag $\delta^{18}O_b$ by 3 kyr similar to the $\delta^{13}C_b$ and %NCW record in the 100-kyr world (Figure S3 and Table S1) whereas $\%CaCO_3$ lags $\delta^{18}O_b$ by 8 kyr.

Moving forward we combine all B/Ca records from this study (DSDP 607; CHN82-24-23PC) and previous studies (DSDP 607, BOFS 8K, MD95-2039, and MD01-2446) from the deep North Atlantic to produce a composite Atlantic B/Ca record. (Figure 4d). Applying the calibration of Yu and Elderfield (2007) yields a long-term change in ΔCO_3^{2-} of 20 μmol/kg with a G/IG amplitude shift of 23 μmol/kg prior to the MPT (1,000–1,500 ka) and 38 μmol/kg post MPT (0–750 ka; Figure 5d; calibration uncertainty ±9 μmol/kg).

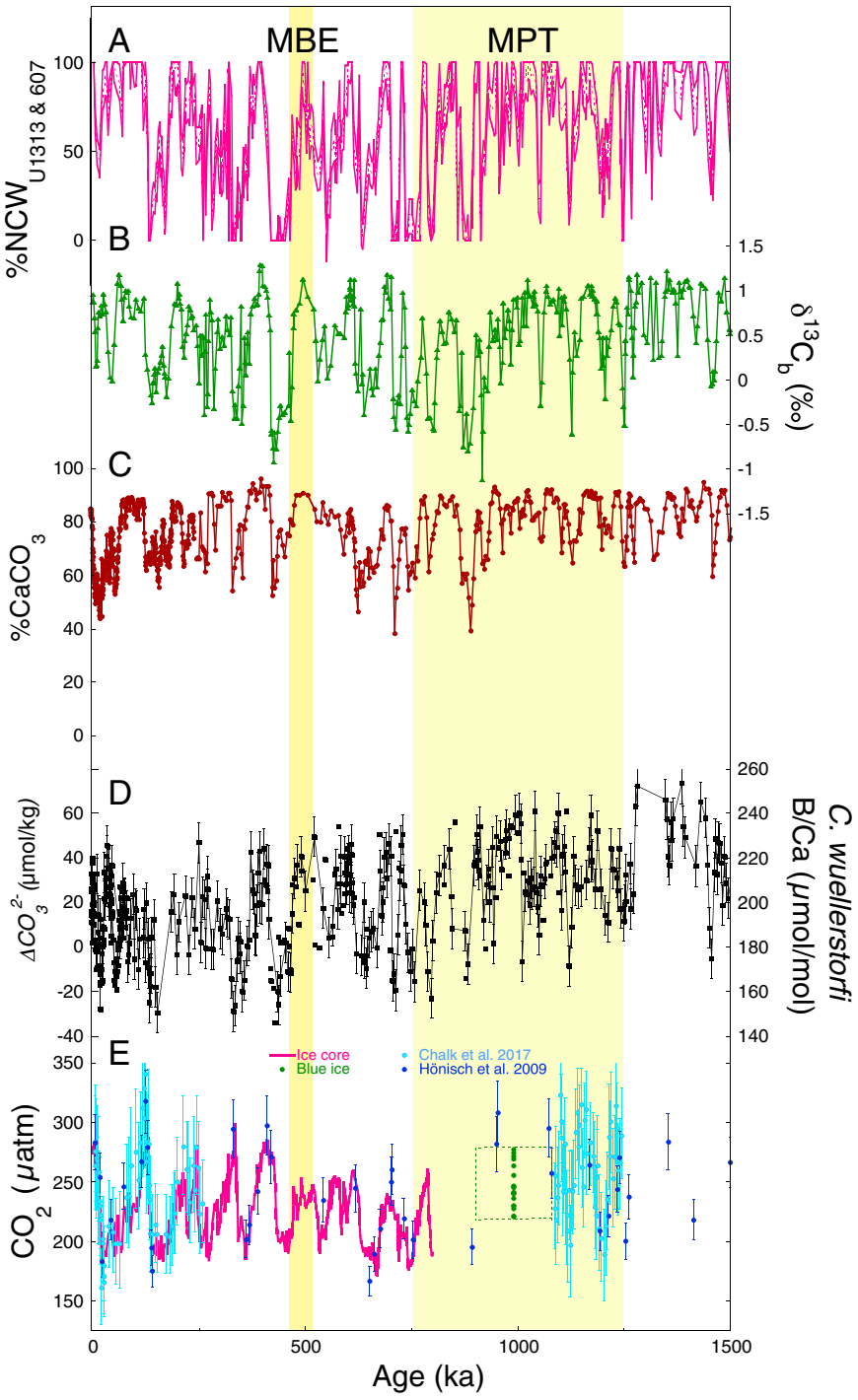

Figure 5. Deep Sea Drilling Program (DSDP) Site 607 (a) %NCW at Site 607 and the re-occupation Site U1313 plotted with 95% confidence intervals (Lang et al., 2016; Raymo et al., 1997) (b) $\delta^{13}C_b$ (Ruddiman et al., 1989), (c) %$CaCO_3$ from DSDP Site 607 and VM30-97 (Ruddiman et al., 1989), (d) compiled deep North Atlantic ocean B/Ca and ΔCO_3^{2-} from DSDP 607 and CHN82–24-23PC and others (Lear et al., 2016; Yu et al., 2008, 2016), and (e) CO_2 reconstructions from ice cores (Bereiter et al., 2015; Luethi et al., 2008; Petit et al., 1999; Siegenthaler et al., 2005), blue ice (Higgins et al., 2015), and boron isotopes (Chalk et al., 2017; Hönisch et al., 2009). The error bars show ΔCO_3^{2-} uncertainty window of ±9 µmol/kg from Yu and Elderfield (2007) calibration. The boxes around the 1 Ma data indicate an age uncertainty of ±89 kyr as presented in Higgins et al. (2015). The mid-Brunhes event and mid-Pleistocene transition are denoted as MBE and MPT.

Interglacial ΔCO_3^{2-} values decrease by 10 μmol/kg from the pre-MPT to post-MPT with average interglacial levels of the last four cycles similar or slightly higher than modern ΔCO_3^{2-} of 33 μmol/kg at Site 607. Glacial ΔCO_3^{2-} levels decreased by 27 μmol/kg from pre-MPT to post-MPT conditions. Our ΔCO_3^{2-} record shows distinct variations on G/IG timescales indicating modifications in deep North Atlantic Ocean carbon storage across the Pleistocene. The range of deepwater ΔCO_3^{2-} variability (>30 μmol/kg), recorded at Site 607, exhibits changes beyond the modern ΔCO_3^{2-} range of the NADW and AABW end-members suggesting that in addition to shifts in water mass distribution, other processes (discussed section 4.1) are driving the observed G/IG cycles in ΔCO_3^{2-}.

Changes in $CaCO_3$ content in deep North Atlantic sediments have been variably related to changes in biological production at the surface, dissolution/preservation on the seafloor, and dilution by terrigenous inputs (Ruddiman et al., 1989). LGM $CaCO_3$ content in various sites in the deep Atlantic has been variably linked to lower $CaCO_3$ production and higher dissolution alongside a higher terrigenous input (Barker, Kiefer, & Elderfield, 2004; Crowley, 1983; Francois & Bacon, 1991; Francois et al., 1990; Sexton & Barker, 2012). However, at Site 607 the ΔCO_3^{2-} records change in parallel with $\%CaCO_3$ suggesting that ΔCO_3^{2-} ion variations are largely associated with the dissolution and preservation cycles in the deep North Atlantic (Figure 5). Deep Atlantic ΔCO_3^{2-} values observed across the Pleistocene are consistent with Atlantic carbonate preservation records showing high preservation during interglacials and enhanced dissolution during glacials (Crowley, 1983; Ruddiman et al., 1989; Sexton & Barker, 2012). Below (see section 4.2), we further explore the relationship between $CaCO_3$ preservation dissolution cycles and deep ocean ΔCO_3^{2-} content.

4. Discussion

4.1. Atlantic Deep Ocean ΔCO_3^{2-} Evolution

Benthic $\delta^{13}C$ in the deep North Atlantic varies in response to changes in the amount of organic carbon/nutrient, the influence of NADW, air-sea gas exchange, and shifts in mean ocean $\delta^{13}C$ (Raymo et al., 1997, 2004). In present day, Site 607 is bathed by NADW, a well-ventilated water mass with high $\delta^{13}C_b$ (>1.0‰) and in saturated conditions (ΔCO_3^{2-} = 33 μmol/kg). In comparison, southern sourced water mass, AABW, is relatively undersaturated (ΔCO_3^{2-} = 0 μmol/kg) and has lower $\delta^{13}C_b$ (~0.4‰) due to higher nutrient content. The ΔCO_3^{2-} and $\delta^{13}C_b$ records closely covary across the last 1 Myr and display similar shifts during the 1,000 to 800 ka interval, thereby suggesting that waxing and waning of northern and southern component waters (SCW) played a key role in deep Atlantic ΔCO_3^{2-} as previously proposed for the LGM and recently for the Pleistocene (Lear et al., 2016; Marchitto et al., 2005; Yu et al., 2008; Figure 5). Pena and Goldstein (2014), using ε_{Nd} proxy, show a decrease in the relative proportion of NADW versus southern sourced water from 1,000 to 900 ka, supporting the notion of a greater contribution of Southern Component Water (SCW) at Site 607. However, the benthic $\delta^{13}C$ and ΔCO_3^{2-} composition of source waters is also impacted by air-sea exchange driven by temperature, and CO_2 outgassing and invasion in the Southern Ocean and North Atlantic (Lynch-Stieglitz et al., 1995). Considering the impact of air-sea gas exchange across the MPT, Lear et al. (2016) estimated that the increase in $\delta^{13}C_b$ partially reflects reduction of outgassing due to an increase in sea ice extent in the Southern Ocean leading to a decline in SCW $\delta^{13}C$ and ΔCO_3^{2-} alongside the increase in SCW at expense of Northern Component Water (NCW) at Site 607.

The decrease in $\delta^{13}C_b$ from 1,000 to 800 ka is associated with a decrease in ΔCO_3^{2-}, which suggests that the incursions of SCW were associated with lower ΔCO_3^{2-} and increased nutrient content, supported by higher Cd/Ca during glacials from a reconstruction at Site 607 (Lear et al., 2016). To examine this further and determine whether this reflects changes in corrosivity of southern sourced deep waters or changes in the volume of SCW, we compare our ΔCO_3^{2-} record to a %NCW record (Lang et al., 2016; Raymo et al., 1997; Figures 5a and 5d). The %NCW record documents the circulation component at Site 607 scaled in terms of relative changes in preformed $\delta^{13}C_b$ composition of NADW (Ocean Drilling Program [ODP] Site 982) and $\delta^{13}C_b$ composition of deep Pacific (ODP Site 849).

From 1,000 to 800 ka, the glacial decrease evident in the ΔCO_3^{2-} record, with a pronounced decline mirrored in both the decrease of $\delta^{13}C_b$ and %NCW record, suggests an increase in SCW penetration to this site, as supported by ε_{Nd} records from Pena and Goldstein (2014). Pleistocene vertical $\delta^{13}C_b$ gradients between intermediate and deep waters in the South Atlantic show that since 1,100 ka, a sharp chemocline

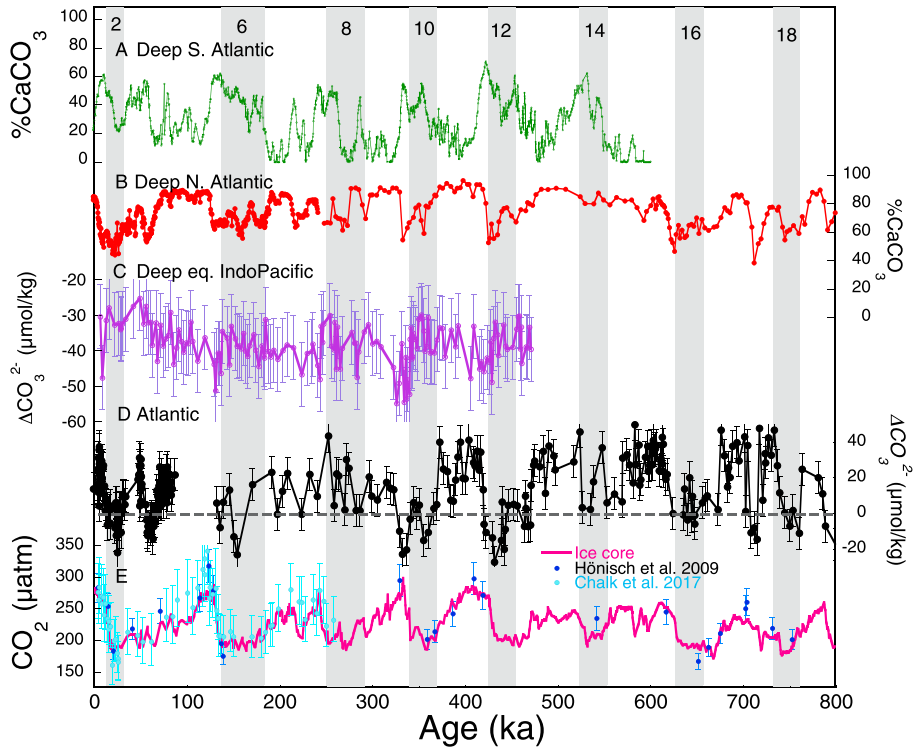

Figure 6. $\%CaCO_3$ records from (a) Ocean Drilling Program 1089 (Hodell et al., 2001) in the deep South Atlantic representing the deep Pacific and (b) Deep Sea Drilling Program 607 and VM30-97 (Ruddiman et al., 1989) in the deep North Atlantic alongside B/Ca-based ΔCO_3^{2-} reconstruction from the (c) equatorial Indo-Pacific (core TT013-PC72; Kerr et al., 2017) and (d) compiled deep North Atlantic ΔCO_3^{2-} with (e) CO_2 reconstructions derived from ice core (Bereiter et al., 2015; Luethi et al., 2008; Petit et al., 1999; Siegenthaler et al., 2005) and B-isotopes (Hönisch et al., 2009; Chalk et al., 2017). The dashed line on panel d represents 0 μmol/kg. The error bars show ΔCO_3^{2-} uncertainty window of ±9 μmol/kg from Yu and Elderfield (2007) calibration.

developed between middepth and deep waters during glacial periods. This sharp chemocline separated well-ventilated intermediate waters from poorly ventilated deep waters (Hodell et al., 2003) consistent with the decrease in ΔCO_3^{2-} recorded at Site 607. Using a stacked magnetic susceptibility record Schmieder et al. (2000) show that during the MPT interim state (from 900 to 600 ka), $CaCO_3$ accumulation rates in the subtropical South Atlantic are notably reduced suggesting greater influence of Antarctic bottom waters. Using planktonic foraminifera fragmentation index, Groger et al. (2003) show the enhancement of G/IG preservation and dissolution cycles at that time. These lines of evidence indicate that changes in our B/Ca-ΔCO_3^{2-} record across the MPT are related to an increase of SCW at the expense of NCW.

Following the MPT, from MIS 20 to 14, both records show similar shifts in glacial values with glacial ΔCO_3^{2-} increasing until MIS 12 paralleling the increase in glacial $\delta^{13}C_b$ values. Interglacial ΔCO_3^{2-} slightly increase from MIS 21 to 17 and then plateau in tandem with the interglacial $\delta^{13}C_b$ trend (Figures 4 and 5). Both features suggest a tight coupling on G/IG timescales. In contrast, the %NCW record shows only a small (~10%) increase in glacial maxima across this time interval. Thus, the inferred small decrease in the volumetric contribution of SCW likely contributed negligibly to the increase in ΔCO_3^{2-} during this time interval. Instead, the close correspondence between the glacial increase in ΔCO_3^{2-} (by about 20 μmol/kg) and the increase in glacial $\delta^{13}C_b$ suggests that both were driven by whole ocean changes in carbon. From MIS 15 onward, Lear et al. (2016) propose that the interglacial increase in $\delta^{13}C_b$ is related to reduced interglacial CO_2 evasion into North Atlantic source waters, impacting both the $\delta^{13}C_b$ and ΔCO_3^{2-} records. Following the MPT, ΔCO_3^{2-} remains at relatively similar levels, suggesting that air-sea gas exchange minimally impacted the interglacial ΔCO_3^{2} North Atlantic source waters (Figure 4).

Stacked planktic and benthic $\delta^{13}C$ foraminifera records show a decrease by 0.35‰ around 900 ka, gradual return to pre-1 Ma values at 500 ka and a final rapid decrease at 420 ka (Hoogakker et al., 2006; Lisiecki,

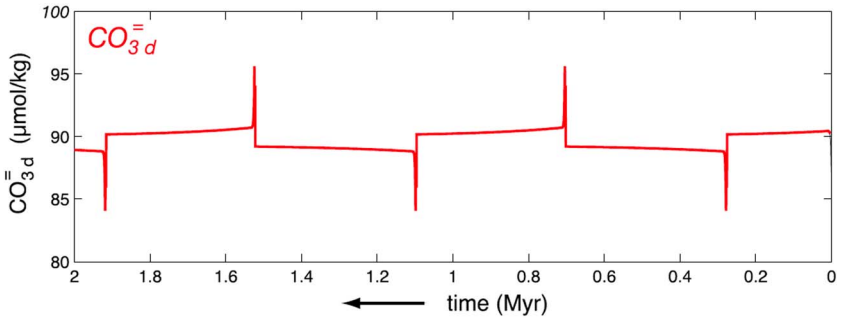

Figure 7. Deep CO_3^{2-} cycles across the Pleistocene as estimated by a seven-box model presented in Toggweiler (2008; see Figure 4) showcasing the classic $CaCO_3$ compensation mechanism. Note that the time axis is inverted.

2010; Wang et al., 2003). The global long-term increase of 0.6 per mil lasting until 500 ka and the subsequent decrease at MIS 12 likely reflect changes in carbon burial to the deep ocean modified by changes in the rain ratio, bottom water ventilation, and surface ocean production (Hoogakker et al., 2006; Lisiecki, 2010; Wang et al., 2003). The similarity between the ΔCO_3^{2-} and $\delta^{13}C_b$ records in both the long-term trends and G/IG variability throughout this time window suggests that it is recording changes in oceanic carbon-carbonate system and changes in deep ocean circulation.

4.2. Deep Ocean CO_3^{2-} and $CaCO_3$ Preservation/Dissolution Cycles

A recent study, using orbitally resolved Indo-Pacific B/Ca records, shows that over the past 500 kyr, deep Pacific ΔCO_3^{2-} G/IG variability parallels changes in sediment $\%CaCO_3$ content, apparently in contrast with the expectation of anticorrelation between these properties derived from the classic compensation theory (Kerr et al., 2017). To explain the apparent contradiction between the expectation from the compensation theory and their observed records, Kerr et al. (2017) argue that a global increase in CO_3^{2-} during glacial intervals is caused by the delivery of alkalinity from the shelves due to the reduction of carbonate deposition on the shelves during low sea level stands (a.k.a. coral reef hypothesis) across the last 450 kyr (Berger, 1982; Opdyke & Walker, 1992). Here we propose an alternative mechanism, whereby the post-MPT Pacific and Atlantic CO_3^{2-} records are driven by basin-to-basin alkalinity transfer, rather than the classic vertical $CaCO_3$ compensation.

Over the past 400 kyr, the Atlantic ΔCO_3^{2-} record shows G/IG swings of 30–40 μmol/kg in the 100-kyr band, which decline into the glacial and recover across the terminations (Figures 5d and 6d). In contrast, the Indo-Pacific records show smaller (<10 μmol/kg) changes in ΔCO_3^{2-} as reported by Kerr et al. (2017) (Figure 6c), which rise into the glacial and shoot down across the terminations. This behavior is also evident in the $\%CaCO_3$ records from the Atlantic, Indo-Pacific, and Southern Ocean, in support of our deep ocean ΔCO_3^{2-} records (Figures 5c, 6a, and 6b). The nature of the deep ocean ΔCO_3^{2-} records contrasts the expected changes as estimated from box models and predicted by $CaCO_3$ compensation theory (Boyle, 1988; Broecker & Peng, 1989; Toggweiler, 1999, 2008).

Using a seven-box model Toggweiler (2008), estimates that in response to deep ocean ventilation the expected change in whole ocean ΔCO_3^{2-} below 1000 m, is on the order of ~9 μmol/kg, significantly lower than ΔCO_3^{2-} swings observed at DSDP Site 607 across the last 400 kyr (Figure 7). Also, the structure of the observed ΔCO_3^{2-} changes lacks the expected spike up on the terminations and down on glacial initiations followed by rapid return to the steady state baseline as expected from the classic compensation theory. Additionally, the large swings in Atlantic ΔCO_3^{2-} are not compensated quickly as expected and the deep Atlantic CO_3^{2-} remains above or below its long-term mean for periods substantially greater than the assumed response time of ~5–10 kyr (Figures 5d and 6d; Archer et al., 1997; Broecker & Peng, 1987; Keir, 1988; Köhler & Fischer, 2006). It is noteworthy that the ΔCO_3^{2-} reconstructions show that both the deep Atlantic and Pacific were undersaturated with respect to calcite during glacial intervals suggesting that dissolution was not the only control on $CaCO_3$ preservation in the deep glacial ocean. The difference in the structure of G/IG change, magnitude, and relative timing between the Atlantic and Pacific deep ΔCO_3^{2-} records questions the classic view of $CaCO_3$ compensatory mechanism and calls for a different approach (Toggweiler, 1999, 2008).

We propose that over the past ~1 Myr, $CaCO_3$ compensation occurred in response to changes in the places where $CaCO_3$ is buried rather than vertical shifts in the lysocline. This explains the Atlantic-Pacific difference and the contrast to the box model predictions. We hypothesize that deep ocean ΔCO_3^{2-} and $\%CaCO_3$ were driven by changes in corrosivity of the deep North Atlantic and interbasin migration of calcite burial or "hot spots" across G/IG cycles (Dunne et al., 2012). A hot spot is an area of the ocean where the enhanced production of $CaCO_3$ at the surface overlies a favorable burial environment on the seafloor. The net result is a local burial flux of $CaCO_3$ that is higher than average. The concept is important because the cumulative burial in a few large hot spots could, in principle, balance the delivery of Ca^{2+} and HCO_3^- ions to the ocean from rivers. At present, the main hot spot or locus of $CaCO_3$ burial is in the deep Atlantic and much of the global burial of $CaCO_3$ occurs there due to the formation of the youngest, least corrosive deep waters in this region (see Figure 1c in Dunne et al., 2012). In contrast, the Pacific Ocean has a less propensity for $CaCO_3$ burial due to the oldest, undersaturated deep waters residing there. Also, in the present day the production and flux of $CaCO_3$ to the seafloor is not uniform across the ocean and burial of $CaCO_3$ is more of a kinetic process than a purely equilibrium process (Broecker & Peng, 1982; Dunne et al., 2012; Li et al., 1969). In this sense, favorable burial environments can also include areas where the water above the seafloor is mildly undersaturated with respect to calcite and enhanced fluxes of $CaCO_3$ to the seafloor overwhelm the dissolution in the sediments (due to the slow kinetics of the dissolution reactions). This nonuniformity, we claim, creates the potential for hot spots of $CaCO_3$ burial and preservation, which result when enhanced fluxes to the seafloor coincide with a relatively shallow seafloor and/or the presence of NADW. In this instance, all the $CaCO_3$ production in areas outside the hot spots tends to dissolve.

Here we build upon these observations and propose that incursion of dense corrosive waters from the southern hemisphere into the glacial deep Atlantic decreased Atlantic calcite burial thus raising the ocean's average CO_3^{2-}. We propose that this is compensated by a shift in the locus of $CaCO_3$ burial into the equatorial Pacific to compensate for the declining burial in the other areas. This is exhibited during glacials, when ΔCO_3^{2-} and $\%CaCO_3$ records show an increase in glacial deep Atlantic corrosivity and undersaturation that inhibits burial across the last 800 kyr (e.g., MIS 12; Figures 6b and 6d). Also, at the same time, empirically, it seems that the locus of burial shifts to the tropical Pacific evident from sedimentary carbonate records, which shows that the area of $CaCO_3$-rich sediments expands in the Pacific during the LGM and shrinks everywhere else (Catubig et al., 1998; Farrell & Prell, 1989). This suggests that the Pacific became a hot spot for $CaCO_3$ burial despite the undersaturated state during glacials. We propose that this is likely caused by the following effects: (i) increase in $CaCO_3$ export that overcame the apparent corrosivity of the water and (ii) the depth at which major $CaCO_3$ dissolution starts is not $\Delta CO_3^{2-} = 0$ but in fact lower. This is consistent with Subhas et al. (2017), suggesting that $CaCO_3$ dissolution starts only at a saturation state of 0.7 not 1. Therefore, it seems that the small increase in deep Pacific ΔCO_3^{2-} was sufficient to shift the balance from carbonate dissolution to preservation. In this way, the ΔCO_3^{2-} in the deep Indo-Pacific rises in response to the same mechanism that keeps the ΔCO_3^{2-} in the deep Atlantic low and the atmospheric pCO_2 low.

When the locus of burial shifts to the Pacific, the ocean's average CO_3^{2} and alkalinity of the ocean must increase to compensate or rise to a point where the burial in the new hot spot is sufficiently high to overcome the general corrosivity of the deep Pacific. These excursions lead to a larger compensation response that is spread out over longer periods of time and would make the amount of alkalinity and dissolved inorganic carbon in the ocean swing widely over time. This is reflected in the slow rise of ΔCO_3^{2-} through stages 4, 3, and 2 in TT013-PC72 (Kerr et al., 2017) and in the late glacial increases in $\%CaCO_3$ at Site 1089, a stand in for burial in the Indo-Pacific (Figure 6a). The gradual increase in alkalinity over this time helps keep the pCO_2 of the atmosphere low for tens of thousands of years and the ocean cold, which reinforces the stratification of the deep Atlantic at times when the ΔCO_3^{2-} falls over time at Site 607 as seen particularly well during MIS 12 and 10. So instead of the CO_3^{2-} simply ticking up and down within a G/IG transition, as in the classical response, a shift of the locus of $CaCO_3$ burial tends to hold the deep CO_3^{2-} up or down over entire glacials or interglacials.

Conversely, when the locus of burial shifts back to the Atlantic during interglacials, the ocean's average CO_3^{2} and alkalinity of the ocean fall because it is suddenly easy to bury $CaCO_3$ again in the less corrosive Atlantic. This seems to be seen especially well during Terminations II and I at VM 28-122 in Yu et al. (2013) and in the $\%CaCO_3$ decreases at Site 1089 (Figure 6a). The net loss of alkalinity from the ocean helps keep the atmospheric pCO_2 high and consequently the ocean warm during interglacials. Also, CO_3^{2-} in the deep Atlantic

is "supersaturated" during IG intervals and as such needs to decrease a lot to reach undersaturation and start dissolution as expressed by the large swings in ΔCO_3^{2-} (30–40 μmol/kg).

The response of $\%CaCO_3$ and deep ocean CO_3^{2-} content to variations in the Atlantic meridional overturning circulation (AMOC) strength has been previously explored in several modeling studies (Chikamoto et al., 2008; Yu et al., 2016). Chikamota et al. (2008) show that during an "AMOC shutdown," initiated by a freshwater perturbation, the average carbonate ion concentration in the North Atlantic is reduced by ~37 μmol/kg and the $CaCO_3$ burial flux is reduced in the North Atlantic and increased in the Pacific. In addition, Yu et al. (2016) investigate the influence of AMOC changes on deep Atlantic CO_3^{2-} and show that a weakening of NADW formation leads to a decrease in deep (>3 km) North Atlantic and Equatorial Atlantic CO_3^{2-} by 20–40 μmol/kg. Although these model results provide some justification for our argument at least, the Chikamoto et al. (2008) model results have a negligible effect on atmospheric pCO_2 in contrast to our conjecture that G-I compensation changes played a role in atmospheric pCO_2. We suggest here that their model does not fully incorporate regional production differences in $CaCO_3$ and does not replicate fully the scenario where the burial of $CaCO_3$ shifts from one ocean to another and concomitant G-I changes in pCO_2.

In previous studies it has been argued that sea level variations drive the cycles of $CaCO_3$ burial and dissolution in the ocean and can explain the low-amplitude variations in the Pacific and glacial increase in ΔCO_3^{2-} and covariation in $\%CaCO_3$ and ΔCO_3^{2-} (Kerr et al., 2017; Yu et al., 2013). Kerr et al. (2017) use the broad correlation of the amplitude of glacial increase in CO_3^{2-} with the amplitude of sea level decline as support. In doing so, the authors suggest that shifts in Atlantic ΔCO_3^{2-} are less sensitive to whole ocean carbonate system changes, as past water mass distribution is strong in this region and impacting deep carbon storage. Furthermore, the ΔCO_3 records presented here resemble the $\delta^{13}C_b$ (proxy of carbon storage and circulation) rather than the $\delta^{18}O_b$ record (proxy of ice volume and sea level). This is very pronounced between MIS 20 and 14 and then 12 and 6 when glacial ΔCO_3 follow closely the $\delta^{13}C_b$ (Figure 5). These lines of evidence suggest that changes in carbon storage in the deep Atlantic are tightly coupled to the very thing that is driving the variations in atmospheric CO_2, namely, changes in the ventilation of southern-sourced bottom water. Building on this idea, we argue that hypothesized enhanced preservation, due to alkalinity supplied from the shelf areas during sea level fall, could affect the Atlantic but not enough to overcome the dissolution changes caused by shifts in ventilation/carbon storage. Therefore, we propose that $CaCO_3$ dissolution in the Atlantic was the dominant source of alkalinity to the deep Pacific and hence played the key role in controlling atmospheric pCO_2 across mid-to-late Pleistocene. Indeed, $CaCO_3$ compensation, as viewed from changes in deep water ΔCO_3^{2-}, occurred throughout the past 1.5 Myr and apparently scaled with the changes in atmospheric pCO_2 (Figure 5).

Across the MPT around 1.1 Ma, the classic ("anticorrelated") $CaCO_3$ patterns (i.e., dissolution in Atlantic and preservation in Pacific during glacials) developed. Sexton and Barker (2012) suggest that this was due to the strengthening of deepwater ventilation in the abyssal Pacific during glacials and weakening during IGs, which led to glacial Pacific $CaCO_3$ dissolution to diminish while driving IG Pacific $CaCO_3$ dissolution to intensify. The proposed idea by these authors would, however, let the respired CO_2 in the deep Pacific escape to the atmosphere during glacials. Here we propose an alternative scenario whereby the development of extremely poor ventilation and increased stratification in the deep Atlantic provides a better explanation for the Pleistocene $CaCO_3$ observations and atmospheric pCO_2. Deep ocean cooling starts at Site 607 in the North Atlantic at ~1.2 Ma (Sosdian & Rosenthal, 2009; Ford et al., 2016), while based on the record from ODP Site 1123, the deep glacial Southern Ocean was close to freezing throughout this period (Elderfield et al., 2012). While it is possible that some of the oxygen isotopic change of seawater change that Elderfield et al. (2012) document at the MPT reflects increase salinity, either way the isotope data reflect an increase in the density of the Southern Ocean deep waters with increased stratification and hence weaker ventilation as seen in the last glacial period in the South Atlantic (Adkins & Schrag, 2001). The cooling of deep water at Site 607 (Ford et al., 2016; Sosdian & Rosenthal, 2009) likely reflects increased stratification of the deep Atlantic. A colder ocean led to northward migration of the Antarctic polar fronts and likely resulted in thicker and more expanded southern sea ice (Kemp et al., 2010) that made the deep ocean more saline, more stratified, and less ventilated over time. We propose that the initial cause of the antiphased behavior between the Atlantic and Pacific relates to the deep ocean cooling across the MPT that led to changes in ventilation and drove the deep Atlantic into undersaturation consistent with the appearance of antiphased behavior in $\%CaCO_3$, as pinpointed by Sexton and Barker (2012) at ~1.1 Ma.

Following the cooling at 1.2 Ma, both the $\delta^{13}C_b$ and %NCW decline from 1 to 0.8 Ma highlighting changes in ventilation. The coherency between the $\delta^{13}C_b$ and Atlantic ΔCO_3^{2-} record across the MPT indicates that changes in deep ocean ventilation are driving deep ocean CO_3^{2-} changes (Figures 3 and 5). Thus, across the MPT, we propose that the increase in deep ocean corrosivity led to the development of the classic $CaCO_3$ pattern, whereby the locus of $CaCO_3$ burial shifts to the Pacific during glacials and switches back the Atlantic during interglacials.

4.3. The Mid-Bruhnes Event

Glacial ΔCO_3^{2-} levels drop by ~30 μmol/kg after MIS 14, becoming for the first time undersaturated through the last 1.5 Myr in the deep North Atlantic at MIS 12, when it reaches -20 ± 9 μmol/kg (Figures 5 and 6). This period of corrosive deep waters corresponds with the mid-Brunhes dissolution event, beginning at ~600 ka and lasting for 400 kyr, peaking around ~400 ka (MIS 11), exhibited by records showing enhanced dissolution in the deep ocean occurring in the North Atlantic (Barker et al., 2006; Crowley, 1985; Groger et al., 2003; Jansen et al., 1986), in the Indian Ocean (Bassinot et al., 1994), and in the Pacific (Farrell & Prell, 1989).

The decrease in the saturation in the deep North Atlantic occurs alongside the development of the largest ice sheets of the Pleistocene, cooling of the deep Southern Ocean and North Atlantic (as recorded in ODP Site 1123 and DSDP Site 607; Elderfield et al., 2012; Sosdian & Rosenthal, 2009) and intensification of the 100 kyr cycles in sea level and pCO_2 (Bereiter et al., 2015; Hönisch et al., 2009; Lisiecki & Raymo, 2005). Cooling of the deep Atlantic, which culminated at MIS 12, likely resulted in greater stratification and sluggish ventilation, which enhanced carbon sequestration in the deep Atlantic possible augmented by increased surface ocean productivity (Lawrence et al., 2013).

The %NCW record shows a prolonged period of near 0% levels, the longest duration of reduced NCWs across the last 800 kyr (Figure 5). Records of ocean circulation show exceptionally prolonged (5 kyr) collapse of the Atlantic Meridional Overturning Circulation (Vazquez Riveiros et al., 2013) and increased influence of SCW (Hall & Becker, 2007) at MIS 12 suggesting a longer residence time of seawater in the glacial deep Atlantic. The isolation of these deep waters allowed greater accumulation of respired organic carbon as surface ocean productivity was higher at Site 607/U1313 as indicated by alkenone mass accumulate rates (C_{37} total MAR) and total organic carbon records (Lawrence et al., 2013; Stein et al., 2009). Both records indicate higher surface ocean productivity possibly tied to the more southerly position of the polar front and/or increased dust supply (Lawrence et al., 2013; Stein et al., 2009).

Modeling studies show that a 50% NADW reduction leads to a decrease of ~30 μmol/kg in the deep Atlantic (>3 km) and NADW cessation leads to a greater decrease of 20–40 μmol/kg (Yu et al., 2016). We propose here that additional decrease in ΔCO_3^{2-} minima starting at MIS 12 sets the stage for the high pCO_2 levels at the mid-Bruhnes event via an increase in whole ocean alkalinity followed by enhanced $CaCO_3$ preservation at MIS 11, 9, and 5. Specifically, we propose that whole ocean alkalinity became higher than "normal" during MIS 12, in response to cooling and reduced ventilation of the deep Atlantic, which caused increase corrosivity. Then, when the deep ocean became better ventilated during termination V, more $CaCO_3$ was preserved everywhere for a short period of time. The enhanced removal of alkalinity then pushed the atmospheric pCO_2 higher. The larger response time than previously assumed contributes to this effect (i.e., the excess alkalinity is not completely removed during the deglaciation but throughout the interglacial maintaining the high pCO_2 levels). This suggests that IG pCO_2 levels are partly determined by the preceding G/IG changes and the response time of the compensation. A noteworthy corollary of the proposed mechanism is that the lower limit of the glacial pCO_2, which has been ~180 ppmV during the past 800 kyr, is not strictly set by the ocean alkalinity, and consequently, the "extra" alkalinity generated at the corrosive glacials (MIS 11, 9, and 5) was available for removal during the subsequent interglacials (e.g., MIS 11, 9, and 5) leading to higher pCO_2 levels.

5. Conclusions

To understand the nature of the ocean's buffering capacity and its role in modulating atmospheric pCO_2, reconstructions of the deep ocean carbonate system parameters are necessary.

Pleistocene benthic foraminiferal B/Ca record from DSDP Site 607 suggests 30–40 μmol/kg G/IG variability in deep ocean ΔCO_3^{2-}, substantially larger than seen in the Indo-Pacific records. The observed timing,

magnitude, and structure of swings in G/IG deep Atlantic ocean ΔCO_3^{2-} are also larger than expected based on thermodynamic $CaCO_3$ compensation mechanism. To explain this difference, we suggest that during glacials, when ventilation weakens, the more corrosive and lower ΔCO_3^{2-} in the deep Atlantic shifts the locus of $CaCO_3$ burial to the equatorial Pacific to maintain the long-term $CaCO_3$ balance via a new carbonate burial hot spot, where the carbonate flux to the seafloor and the small increase in ΔCO_3^{2-} are sufficient to overcome the undersaturated conditions characteristic of the deep Pacific during interglacial intervals. We argue that the small increase in Indo-Pacific ΔCO_3^{2-} is driven by the same mechanism that keeps the deep Atlantic ΔCO_3^{2-} and atmospheric pCO_2 low and is not due to the delivery of alkalinity from the shelves during low sea level stands.

Shifts in the global carbon cycle and deep ocean circulation play a role in driving the long-term trend in Atlantic ΔCO_3^{2-} across the mid-to-late Pleistocene. The ΔCO_3^{2-} record from DSDP Site 607 shows shifts in G/IG variability associated with the MPT and mid-Brunhes event. The shift in the locus of $CaCO_3$ burial likely initiated across the MPT as the deep Atlantic Ocean began to play a large role in enhancing pCO_2 due to changes in ventilation, likely due to cooling and enhanced stratification, which drove the deep Atlantic into undersaturation during glacial intervals. Deep ocean ΔCO_3^{2-} levels reached the lowest levels of the last 1.5 Myr at MIS 12 and became persistently undersaturated. We propose that the low ΔCO_3^{2-} of MIS 12 were possibly initiated by a combination of sluggish circulation and high surface ocean productivity allowing for increased storage of CO_2 in the deep Atlantic. The low ΔCO_3^{2-} of the deep Atlantic set the stage for the high pCO_2 levels at MIS 11 via an increase in whole ocean alkalinity followed by enhanced $CaCO_3$ preservation at MIS 11 and the subsequent interglacials of MIS 9 and 5.

Acknowledgments
Thanks to useful discussions with Phil Sexton, help with time series analysis from Henrieka Detlef and Kira Lawrence, and ICPMS technical support from Paul Field. We also thank anonymous reviewers for comments that greatly improved the manuscript. Sindia Sosdian acknowledges the financial support provided by the Welsh Government and Higher Education Funding Council for Wales through the Sêr Cymru National Research Network for Low Carbon, Energy and Environment. Yair Rosenthal acknowledges NSF support (OCE 1334691). All data presented in this study are given in the supporting information.

References

Adkins, J. F., & Schrag, D. P. (2001). Pore fluid constraints on deep ocean temperature and salinity during the Last Glacial Maximum. *Geophysical Research Letters*, *28*(5), 771–774. https://doi.org/10.1029/2000GL011597

Allen, K. A., Sikes, E. L., Hönisch, B., Elmore, A. C., Guilderson, T. P., Rosenthal, Y., & Anderson, R. F. (2015). Southwest Pacific deep water carbonate chemistry linked to high southern latitude climate and atmospheric CO_2 during the Last Glacial Termination. *Quaternary Science Reviews*, *122*, 180–191. https://doi.org/10.1016/j.quascirev.2015.05.007

Archer, D., Kheshgi, H., & MaierReimer, E. (1997). Multiple timescales for neutralization of fossil fuel CO_2. *Geophysical Research Letters*, *24*(4), 405–408. https://doi.org/10.1029/97GL00168

Archer, D., & Maierreimer, E. (1994). Effect of deep-sea sedimentary calcite preservation on atmospheric CO_2 concentration. *Nature*, *367*(6460), 260–263. https://doi.org/10.1038/367260a0

Arhenius, G. (1952). Sediment cores from the East Pacific. *Reports of the Swedish Deep Sea Expeditions*, *1947-1948*, 1–227.

Babila, T. L., Rosenthal, Y., & Conte, M. H. (2014). Evaluation of the biogeochemical controls on B/Ca of Globigerinoides ruber white from the Oceanic Flux Program, Bermuda. *Earth and Planetary Science Letters*, *404*, 67–76. https://doi.org/10.1016/j.epsl.2014.05.053

Barker, S., Archer, D., Booth, L., Elderfield, H., Henderiks, J., & Rickaby, R. E. M. (2006). Globally increased pelagic carbonate production during the Mid-Brunhes dissolution interval and the CO_2 paradox of the MIS 11. *Quaternary Science Reviews*, *25*(23–24), 3278–3293. https://doi.org/10.1016/j.quascirev.2006.07.018

Barker, S., Kiefer, T., & Elderfield, H. (2004). Temporal changes in North Atlantic circulation constrained by planktonic foraminiferal shell weights. *Paleoceanography*, *19*, PA3008. https://doi.org/10.1029/2004PA001004

Bassinot, F. C., Beaufort, L., Vincent, E., Labeyrie, L. D., Rostek, F., Muller, P. J., et al. (1994). Coarse fraction fluctuations in pelagic carbonate sediments from the tropical Indian Ocean—A 1500-kyr record of carbonate dissolution. *Paleoceanography*, *9*(4), 579–600. https://doi.org/10.1029/94PA00860

Bereiter, B., Eggleston, S., Schmitt, J., Nehrbass-Ahles, C., Stocker, T. F., Fischer, H., et al. (2015). Revision of the EPICA Dome C CO_2 record from 800 to 600 kyr before present. *Geophysical Research Letters*, *42*, 542–549. https://doi.org/10.1002/2014gl061957

Berger, W. H. (1982). Increase of carbon dioxide in the atmosphere during deglaciation: The coral reef hypothesis. *Naturwissenschaften*, *69*(2), 87–88. https://doi.org/10.1007/BF00441228.

Berger, W. H., & Keir, R. S. (1984). Glacial-Holocene changes in atmospheric CO_2 and the deep-sea record. In J. E. Hansen & T. Takahashi (Eds.), *Climate Processes and Climate Sensitivity*, *Geophysical Monograph Series* (Vol. 29, pp. 337–351). Washington, DC: American Geophysical Union. https://doi.org/10.1029/GM029p0337

Berger, W. H., & Winterer, E. L. (1974). Plate stratigraphy and the fluctuating carbonate line. In K. J. Hsu & H. C. Jeakyns (Eds.), *Pelagic Sediments on Land and Under the Sea*, *Spec. Publ. Int. Assoc. Sedimentol.* (Vol. 1, pp. 11–48).

Boyle, E. A. (1983). Chemical accumulation variations under the Peru current during the past 130,000 years. *Journal of Geophysical Research*, *88*(C12), 7667–7680.

Boyle, E. A. (1988). Vertical oceanic nutrient fractionation and glacial-interglacial CO_2 cycles. *Nature*, *331*(6151), 55–56. https://doi.org/10.1038/331055a0

Boyle, E. A., & Keigwin, L. (1985). Comparison of Atlantic and Pacific paleochemical records for the last 215,000 years—Changes in deep ocean circulation and chemical inventories. *Earth and Planetary Science Letters*, *76*(1-2), 135–150. https://doi.org/10.1016/0012-821X(85)90154-2

Broecker, W. S., & Peng, T. H. (1987). The role of $CaCO_3$ compensation in the glacial to interglacial atmospheric CO_2 change. *Global Biogeochemical Cycles*, *1*(1), 15–29. https://doi.org/10.1029/GB001i001p00015

Broecker, W. S., & Peng, T.-H. (1982). *Tracers in the sea*. Palisades, New York: Lamont-Doherty Geol. Obs.

Broecker, W. S., & Peng, T.-H. (1989). The cause of the glacial to interglacial CO2 change: a polar alkalinity hypothesis. *Global Biogeochemical Cycles*, *3*, 215–239.

Brown, R. E., Anderson, L. D., Thomas, E., & Zachos, J. C. (2011). A core-top calibration of B/Ca in the benthic foraminifers Nuttallides umbonifera and Oridorsalis umbonatus: A proxy for Cenozoic bottom water carbonate saturation. *Earth and Planetary Science Letters*, *310*(3–4), 360–368. https://doi.org/10.1016/j.epsl.2011.08.023

Catubig, N. R., Archer, D. E., Francois, R., deMenocal, P., Howard, W., & Yu, E.-F. (1998). Global deep-sea burial rate of calcium carbonate during the Last Glacial Maximum. *Paleoceanography*, *13*(3), 298–310. https://doi.org/10.1029/98PA00609

Chalk, T. B., Hain, M. P., Foster, G. L., Rohling, E. J., Sexton, P. F., Badger, M. P. S., et al. (2017). Causes of ice age intensification across the mid-Pleistocene transition. *Proceedings of the National Academy of Sciences of the United States of America*, *114*(50), 13,114–13,119. https://doi.org/10.1073/pnas.1702143114

Chikamoto, M. O., Matsumoto, K., & Ridgwell, A. (2008). Response of deep-sea $CaCO_3$ sedimentation to Atlantic meridional overturning circulation shutdown. *Journal of Geophysical Research*, *113*, G03017. https://doi.org/10.1029/2007JG000669

Clark, P. U., Archer, D., Pollard, D., Blum, J. D., Rial, J. A., Brovkin, V., et al. (2006). The middle Pleistocene transition: Characteristics. Mechanisms, and implications for long-term changes in atmospheric pCO_2. *Quaternary Science Reviews*, *25*(23–24), 3150–3184. https://doi.org/10.1016/j.quascirev.2006.07.008

Crowley, T. J. (1983). Calcium-carbonate preservation patterns in the central North Atlantic during the last 150,000 years. *Marine Geology*, *51*(1–2), 1–14. https://doi.org/10.1016/0025-3227(83)90085-3

Crowley, T. J. (1985). Late Quaternary carbonate changes in the North Atlantic and Atlantic/Pacific comparisons. In E. T. Sundquist & W. S. Broecker (Eds.), *The Carbon Cycle and Atmospheric CO_2: Natural Variations. Archean to Present* (pp. 271–284). Washington, DC: American Geophysical Union.

deMenocal, P., Archer, D., & Leth, P. (1997). Pleistocene variations in deep Atlantic circulation and calcite burial between 1.2–0.6 Ma: A combined data-model approach, Proceedings of the Ocean Drilling Program. *Scientific Results*, *154*, 285–297.

Doss, W., & Marchitto, T. M. (2013). Glacial deep ocean sequestration of CO_2 driven by the eastern equatorial Pacific biologic pump. *Earth and Planetary Science Letters*, *377*, 43–54.

Dunne, J. P., Hales, B., & Toggweiler, J. R. (2012). Global calcite cycling constrained by sediment preservation controls. *Global Biogeochemical Cycles*, *26*, GB3023. https://doi.org/10.1029/2010GB003935

Elderfield, H., Ferretti, P., Greaves, M., Crowhurst, S., McCave, I. N., Hodell, D., & Piotrowski, A. M. (2012). Evolution of ocean temperature and ice volume through the mid-Pleistocene climate transition. *Science*, *337*(6095), 704–709. https://doi.org/10.1126/science.1221294

Elmore, A. C., McClymont, E. L., Elderfield, H., Kender, S., Cook, M. R., Leng, M. J., et al. (2015). Antarctic Intermediate Water properties since 400 ka recorded in infaunal (Uvigerina peregrina) and epifaunal (Planulina wuellerstorfi) benthic foraminifera. *Earth and Planetary Science Letters*, *428*, 193–203. https://doi.org/10.1016/j.epsl.2015.07.013

Farrell, J. W., & Prell, W. L. (1989). Climatic change and $CaCO_3$ preservation: An 800,000 year bathymetric reconstruction from central equatorial Pacific Ocean. *Paleoceanography*, *4*(4), 447–466. https://doi.org/10.1029/PA004i004p00447

Ford, H., Sosdian, S. M., Rosenthal, Y., & Raymo, M. E. (2016). Gradual and abrupt changes during the mid-Pleistocene transition. *Quaternary Science Reviews*, *149*, 222–233.

Francois, R., & Bacon, M. P. (1991). Variations in terrigenous input into the deep equatorial Atlantic during the past 24,000 years. *Science*, *251*(5000), 1473–1476. https://doi.org/10.1126/science.251.5000.1473

Francois, R., Bacon, M. P., & Suman, D. O. (1990). Thorium-230 profiling in deep sea sediments: High resolution records of flux and dissolution of carbonate in the equatorial Atlantic during the last 24,000 years. *Paleoceanography*, *5*(5), 761–787. https://doi.org/10.1029/PA005i005p00761

Groger, M., Henrich, R., & Bickert, T. (2003). Glacial-interglacial variability in lower North Atlantic deep water: Inference from silt grain-size analysis and carbonate preservation in the western equatorial Atlantic. *Marine Geology*, *201*(4), 321–332. https://doi.org/10.1016/S0025-3227(03)00263-9

Hain, M. P., Sigman, D. M., & Haug, G. H. (2010). Carbon dioxide effects of Antarctic stratification, North Atlantic Intermediate Water formation, and subantarctic nutrient drawdown during the last ice age: Diagnosis and synthesis in a geochemical box model. *Global Biogeochemical Cycles*, *24*, GB4023. https://doi.org/10.1029/2010GB003790

Hall, I. R., & Becker, J. (2007). Deep Western Boundary Current variability in the subtropical northwest Atlantic Ocean during marine isotope stages 12–10. *Geochemistry, Geophysics, Geosystems*, *8*, Q06013. https://doi.org/10.1029/2006GC001518

Higgins, J. A., Kurbatov, A. V., Spaulding, N. E., Brook, E., Introne, D. S., Chimiak, L. M., et al. (2015). Atmospheric composition 1 million years ago from blue ice in the Allan Hills, Antarctica. *Proceedings of the National Academy of Sciences of the United States of America*, *112*(22), 6887–6891. https://doi.org/10.1073/pnas.1420232112

Hodell, D. A., Charles, C. D., & Sierro, F. J. (2001). Late Pleistocene evolution of the ocean's carbonate system. *Earth and Planetary Science Letters*, *192*(2), 109–124. https://doi.org/10.1016/S0012-821X(01)00430-7

Hodell, D. A., Venz, K. A., Charles, C. D., & Ninnemann, U. S. (2003). Pleistocene vertical carbon isotope and carbonate gradients in the South Atlantic sector of the Southern Ocean. *Geochemistry, Geophysics, Geosystems*, *4*(1), 1004. https://doi.org/10.1029/2002GC000367

Hönisch, B., Hemming, N. G., Archer, D., Siddall, M., & McManus, J. F. (2009). Atmospheric carbon dioxide concentration across the mid-Pleistocene transition. *Science*, *324*(5934), 1551–1554. https://doi.org/10.1126/science.1171477

Hoogakker, B. A. A., Rohling, E. J., Palmer, M. R., Tyrrell, T., & Rothwell, R. G. (2006). Underlying causes for long-term global ocean delta C-13 fluctuations over the last 1.20 Myr. *Earth and Planetary Science Letters*, *248*(1–2), 15–29. https://doi.org/10.1016/j.epsl.2006.05.007

Howard, W. R., & Prell, W. L. (1994). Late Quaternary $CaCO_3$ production and preservation in Southern Ocean—Implications of for oceanic and atmospheric carbon cycling. *Paleoceanography*, *9*(3), 453–482. https://doi.org/10.1029/93PA03524

Howe, J. N. W., Piotrowski, A. M., Noble, T. L., Mulitza, S., Chiessi, C. M., & Bayon, G. (2016). North Atlantic Deep Water production during the Last Glacial Maximum. *Nature Communications*, *7*. https://doi.org/10.1038/ncomms11765

Howell, P., Pisias, N., Ballance, J., Baughman, J., & Ochs, L. (2006). *Arand time series analysis software*. Providence, RI: Brown University.

Jansen, J. H. F., Kuijpers, A., & Troelstra, S. R. (1986). A mid-Brunhes climatic event-long term changes in global atmosphere and ocean circulation. *Science*, *232*(4750), 619–622. https://doi.org/10.1126/science.232.4750.619

Keir, R. S. (1988). On the late Pleistocene ocean geochemistry and circulation. *Paleoceanography*, *3*(4), 413–445. https://doi.org/10.1029/PA003i004p00413

Kemp, A. E. S., Grigorov, I., Pearce, R. B., & Naveira Garabato, A. C. (2010). Migration of the Antarctic Polar Front through the mid-Pleistocene transition: Evidence and climatic implications. *Quaternary Science Reviews*, *29*(17-18), 1993–2009. https://doi.org/10.1016/j.quascirev.2010.04.027

Kender, S., McClymont, E. L., Elmore, A. C., Emanuele, D., Leng, M. J., & Elderfield, H. (2016). Mid Pleistocene foraminiferal mass extinction coupled with phytoplankton evolution. *Nature Communications*, *7*. https://doi.org/10.1038/ncomms11970

Kerr, J., Rickaby, R., Yu, J., Elderfield, H., & Sadekov, A. Y. (2017). The effect of ocean alkalinity and carbon transfer on deep-sea carbonate ion concentration during the past five glacial cycles. *Earth and Planetary Science Letters*, *471*, 42–53. https://doi.org/10.1016/j.epsl.2017.04.042

Key, R. M., Kozyr, A., Sabine, C. L., Lee, K., Wanninkhof, R., Bullister, J. L., et al. (2004). A global ocean carbon climatology: Results from Global Data Analysis Project (GLODAP). *Global Biogeochemical Cycles*, *18*, GB4031. https://doi.org/10.1029/2004GB002247

Köhler, P., & Fischer, H. (2006). Simulating low frequency changes in atmospheric CO2 during the last 740 000 years. *Climate of the Past*, *2*, 57–78.

Lang, D. C., Bailey, I., Wilson, P. A., Chalk, T. B., Foster, G. L., & Gutjahr, M. (2016). Incursions of southern-sourced water into the deep North Atlantic during late Pliocene glacial intensification. *Nature Geoscience*, *9*(5), 375–379. https://doi.org/10.1038/ngeo2688

Lawrence, K. T., Sigman, D. M., Herbert, T. D., Riihimaki, C. A., Bolton, C. T., Martinez-Garcia, A., et al. (2013). Time-transgressive North Atlantic productivity changes upon Northern Hemisphere glaciation. *Paleoceanography*, *28*, 740–751. https://doi.org/10.1002/2013PA002546

Lear, C. H., Billups, K., Rickaby, R. E. M., Diester-Haass, L., Mawbey, E., & Sosdian, S. M. (2016). Breathing more deeply: Deep ocean carbon storage during the mid-Pleistocene climate transition. *Geology*, *44*(12), 1035–1038. https://doi.org/10.1130/G38636.1

Lemarchand, D., Gaillardet, J., Lewin, E., & Allegre, C. J. (2002). Boron isotope systematics in large rivers: Implications for the marine boron budget and paleo-pH reconstruction over the Cenozoic. *Chemical Geology*, *190*(1–4), 123–140. https://doi.org/10.1016/S0009-2541(02)00114-6

Li, Y.-H., Takahashi, T., & Broecker, W. S. (1969). Degree of saturation of $CaCO_3$ in the oceans. *Journal of Geophysical Research*, *74*(23), 5507–5525. https://doi.org/10.1029/JC074i023p05507

Lisiecki, L. E. (2010). A benthic delta C-13-based proxy for atmospheric pCO_2 over the last 1.5 Myr. *Geophysical Research Letters*, *37*, L21708. https://doi.org/10.1029/2010GL045109

Lisiecki, L. E., & Raymo, M. E. (2005). A Pliocene-Pleistocene stack of 57 globally distributed benthic delta O-18 records. *Paleoceanography*, *20*, PA1003. https://doi.org/10.1029/2004PA001071

Luethi, D., Lüthi, D., le Floch, M., Bereiter, B., Blunier, T., Barnola, J.-M., et al. (2008). High-resolution carbon dioxide concentration record 650,000–800,000 years before present. *Nature*, *453*(7193), 379–382. https://doi.org/10.1038/nature06949

Lynch-Stieglitz, J., Stocker, T. F., Broecker, W. S., & Fairbanks, R. G. (1995). The influence of air-sea exchange on the isotopic composition of oceanic carbon: Observations and modelling. *Global Biogeochemical Cycles*, *9*(4), 653–665. https://doi.org/10.1029/95GB02574

Marchitto, T. M., Lynch-Stieglitz, J., & Hemming, S. R. (2005). Deep pacific $CaCO_3$ compensation and glacial-interglacial atmospheric CO_2. *Earth and Planetary Science Letters*, *231*(3–4), 317–336. https://doi.org/10.1016/j.epsl.2004.12.024

Opdyke, B. N., & Walker, J. C. G. (1992). Return of the coral-reef hypothesis—Basin to shelf partitioning of $CaCO_3$ and its effect on atmospheric CO_2. *Geology*, *20*(8), 733–736. https://doi.org/10.1130/0091-7613(1992)020%3C0733:ROTCRH%3E2.3.CO;2

Pena, L. D., & Goldstein, S. L. (2014). Thermohaline circulation crisis and impacts during the mid-Pleistocene transition. *Science*, *345*(6194), 318–322. https://doi.org/10.1126/science.1249770

Petit, J. R., Jouzel, J., Raynaud, D., Barkov, N. I., Barnola, J. M., Basile, I., et al. (1999). Climate and atmospheric history of the past 420,000 years from the Vostok ice core, Antarctica. *Nature*, *399*(6735), 429–436. https://doi.org/10.1038/20859

Rae, J. W. B., Foster, G. L., Schmidt, D. N., & Elliott, T. (2011). Boron isotopes and B/Ca in benthic foraminifera: Proxies for the deep ocean carbonate system. *Earth and Planetary Science Letters*, *302*(3–4), 403–413. https://doi.org/10.1016/j.epsl.2010.12.034

Raitzsch, M., Hathorne, E. C., Kuhnert, H., Groeneveld, J., & Bickert, T. (2011). Modern and late Pleistocene B/Ca ratios of the benthic foraminifer Planulina wuellerstorfi determined with laser ablation ICP-MS. *Geology*, *39*(11), 1039–1042. https://doi.org/10.1130/G32009.1

Raymo, M. E., Oppo, D. W., & Curry, W. (1997). The mid-Pleistocene climate transition: A deep sea carbon isotopic perspective. *Paleoceanography*, *12*(4), 546–559. https://doi.org/10.1029/97PA01019

Raymo, M. E., Oppo, D. W., Flower, B. P., Hodell, D. A., McManus, J. F., Venz, K. A., et al. (2004). Stability of North Atlantic water masses in face of pronounced climate variability during the Pleistocene. *Paleoceanography*, *19*, PA2008. https://doi.org/10.1029/2003PA000921

Rickaby, R. E. M., Elderfield, H., Roberts, N., Hillenbrand, C. D., & Mackensen, A. (2010). Evidence for elevated alkalinity in the glacial Southern Ocean. *Paleoceanography*, *25*, PA1209. https://doi.org/10.1029/2009PA001762

Rosenthal, Y., Boyle, E. A., & Labeyrie, L. (1997). Last Glacial Maximum paleochemistry and deepwater circulation in the Southern Ocean: Evidence from foraminiferal cadmium. *Paleoceanography*, *12*(6), 787–796. https://doi.org/10.1029/97PA02508

Rosenthal, Y., Field, M. P., & Sherrell, R. M. (1999). Precise determination of element/calcium ratios in calcareous samples using sector field inductively coupled plasma mass spectrometry. *Analytical Chemistry*, *71*(15), 3248–3253. https://doi.org/10.1021/ac981410x

Ruddiman, W. F., Raymo, M. E., Martinson, D. G., Clement, B. M., & Backman, J. (1989). Pleistocene evolution: Northern hemisphere ice sheets and North Atlantic Ocean. *Paleoceanography*, *4*(4), 353–412. https://doi.org/10.1029/PA004i004p00353

Schlitzer, R. (2012). Ocean Data View. Retrieved from http://odv.awi.de

Schmieder, F., von Dobeneck, T., & Bleil, U. (2000). The mid-Pleistocene climate transition as documented in the deep South Atlantic Ocean: Initiation, interim state and terminal event. *Earth and Planetary Science Letters*, *179*(3–4), 539–549. https://doi.org/10.1016/S0012-821X(00)00143-6

Sexton, P. F., & Barker, S. (2012). Onset of 'Pacific-style' deep-sea sedimentary carbonate cycles at the mid-Pleistocene transition. *Earth and Planetary Science Letters*, *321*, 81–94.

Siegenthaler, U., Stocker, T. F., Monnin, E., Lüthi, D., Schwander, J., Stauffer, B., et al. (2005). Stable carbon cycle-climate relationship during the late Pleistocene. *Science*, *310*(5752), 1313–1317. https://doi.org/10.1126/science.1120130

Sigman, D. M., & Boyle, E. A. (2000). Glacial/interglacial variations in atmospheric carbon dioxide. *Nature*, *407*(6806), 859–869. https://doi.org/10.1038/35038000

Skinner, L. C. (2009). Glacial-interglacial atmospheric CO_2 change: A possible standing volume effect on deep-ocean carbon sequestration. *Climate of the Past*, *5*(3), 537–550. https://doi.org/10.5194/cp-5-537-2009

Sosdian, S., & Rosenthal, Y. (2009). Deep-sea temperature and ice volume changes across the Pliocene-Pleistocene climate transitions. *Science*, *325*(5938), 306–310. https://doi.org/10.1126/science.1169938

Stein, R., Hefter, J., Grutzner, J., Voelker, A., & Naafs, B. D. A. (2009). Variability of surface water characteristics and Heinrich-like events in the Pleistocene midlatitude North Atlantic Ocean: Biomarker and XRD records from IODP Site U1313 (MIS 16–9). *Paleoceanography*, *24*, PA2203. https://doi.org/10.1029/2008PA001639

Subhas, A. V., Adkins, J. F., Rollins, N. E., Naviaux, J., Erez, J., & Berelson, W. M. (2017). Catalysis and chemical mechanisms of calcite dissolution in seawater. *Proceedings of the National academy of Sciences of the United States of America*, *114*(31), 8175–8180. https://doi.org/10.1073/pnas.1703604114

Toggweiler, J. R. (1999). Variation of atmospheric CO_2 by ventilation of the ocean's deepest water. *Paleoceanography*, *14*(5), 571–588. https://doi.org/10.1029/1999PA900033

Toggweiler, J. R. (2008). Origin of the 100,000-year timescale in Antarctica temperatures and atmospheric CO_2. *Paleoceanography*, *23*, PA2211. https://doi.org/10.1029/2006PA001405

Tzedakis, P. C., Raynaud, D., McManus, J. F., Berger, A., Brovkin, V., & Kiefer, T. (2009). Interglacial diversity. *Nature Geoscience*, *2*(11), 751–755. https://doi.org/10.1038/ngeo660

Vazquez Riveiros, N., Waelbroeck, C., Skinner, L., Duplessy, J. C., McManus, J. F., Kandiano, E. S., & Bauch, H. A. (2013). The MIS 11 paradox and ocean circulation: Role of millennial scale events. *Earth and Planetary Science Letters*, *371*, 258–268.

Wang, P. X., Tian, J., Cheng, X. R., Liu, C. L., & Xu, J. (2003). Carbon reservoir changes preceded major ice-sheet expansion at the mid-Brunhes event. *Geology*, *31*(3), 239–242. https://doi.org/10.1130/0091-7613(2003)031%3C0239:CRCPMI%3E2.0.CO;2

Yu, J., Anderson, R. F., Jin, Z., Menviel, L., Zhang, F., Ryerson, F. J., & Rohling, E. J. (2014). Deep South Atlantic carbonate chemistry and increased interocean deep water exchange during last deglaciation. *Quaternary Science Reviews*, *90*, 80–89. https://doi.org/10.1016/j.quascirev.2014.02.018

Yu, J., Anderson, R. F., Jin, Z., Rae, J. W. B., Opdyke, B. N., & Eggins, S. M. (2013). Responses of the deep ocean carbonate system to carbon reorganization during the last glacial-interglacial cycle. *Quaternary Science Reviews*, *76*, 39–52. https://doi.org/10.1016/j.quascirev.2013.06.020

Yu, J., Broecker, W. S., Elderfield, H., Jin, Z., McManus, J., & Zhang, F. (2010). Loss of carbon from the Deep Sea since the Last Glacial Maximum. *Science*, *330*(6007), 1084–1087. https://doi.org/10.1126/science.1193221

Yu, J., & Elderfield, H. (2007). Benthic foraminiferal B/Ca ratios reflect deep water carbonate saturation state. *Earth and Planetary Science Letters*, *258*(1–2), 73–86. https://doi.org/10.1016/j.epsl.2007.03.025

Yu, J., Elderfield, H., & Piotrowski, A. M. (2008). Seawater carbonate ion-delta C-13 systematics and application to glacial-interglacial North Atlantic ocean circulation. *Earth and Planetary Science Letters*, *271*(1–4), 209–220. https://doi.org/10.1016/j.epsl.2008.04.010

Yu, J., Menviel, L., Jin, Z. D., Thornalley, D. J. R., Barker, S., Marino, G., et al. (2016). Sequestration of carbon in the deep Atlantic during the last glaciation. *Nature Geoscience*, *9*(4), 319–324. https://doi.org/10.1038/ngeo2657